INL/CON-10-17975
PREPRINT

Pressure Resistance Welding of High Temperature Metallic Materials

ANS Decomissioning, Decontamination & Reutilization Conference

N. Jerred
L. Zirker
B. Jacques
T. Bradshaw
J. Carrillo
E. Young
I. Charit
J. Cole
M. Frary
D. Butt
M. Meyer
K. L. Murty

The INL is a
U.S. Department of Energy
National Laboratory
operated by
Battelle Energy Alliance

August 2010

Pressure Resistance Welding of High Temperature Metallic Materials

N. Jerred[1], L. Zirker[2], B. Jaques[3], T. Bradshaw[4], J. Carrillo[3], E. Young[3], I. Charit[1], J. Cole[2], M. Frary[3], D. Butt[3], M. Meyer[2], and K.L. Murty[4]

[1] University of Idaho
Moscow, ID USA
[2] Idaho National Laboratory
Idaho Falls, ID USA
[3] Boise State University
Boise, ID USA
[4] North Carolina State University
Raleigh, NC USA

Keywords: Pressure Resistance Welding; Dissimilar Materials Joint; ODS alloys; Advanced Nuclear Reactors

Abstract

Pressure Resistance Welding (PRW) is a solid state joining process used for various high temperature metallic materials (Oxide dispersion strengthened alloys of MA957, MA754; ferritic/martensitic alloy HT-9, and tungsten) for advanced nuclear reactor applications. A new PRW machine has been installed at the Center for Advanced Energy Studies (CAES) in Idaho Falls for conducting joining research for nuclear applications. The key emphasis has been on understanding processing-microstructure-property relationships. Initial studies have shown that sound joints can be made between dissimilar materials such as MA957 alloy cladding tubes and HT-9 end plugs, and MA754 and HT-9 coupons. Limited burst testing of MA957/HT-9 joints carried out at various pressures up to 400^{o}C has shown encouraging results in that the joint regions do not develop any cracking. Similar joint strength observations have also been made by performing simple bend tests. Detailed microstructural studies using SEM/EBSD tools and fatigue crack growth studies of MA754/HT-9 joints are ongoing.

Introduction

Advanced nuclear reactors are being designed and developed to sustain the ever-increasing energy demands of our society. These advanced reactors would require the use of materials exhibiting superior dimensional stability, high strength and toughness, resistance to the onset of creep and creep rupture, and compatibility with the reactor fluids under the reactor environment. For in-reactor operation, the integrity of core largely depends on the performance of the fuel, cladding and core support structures. To meet the materials operational requirements, nickel- and iron-based oxide dispersion strengthened (ODS) alloys, ferritic-martensitic (F-M) alloys and the refractory metal (such as tungsten) could be some of the viable choices [1].

In conventional light water reactors zirconium alloys, mainly used as cladding materials, and stainless steels, used as in-core support structures, exhibit decreased strength at elevated temperatures due to neutron degradation. In high temperature reactor applications, ODS alloys have become attractive due to their elevated temperature strength, overall resistance to creep, and

good radiation tolerance. The improved strength of these alloys is attributed to the stability the dispersed yttria (Y_2O_3) oxide particles provide to the matrix material. These ODS alloys are fabricated via mechanical alloying and subsequent thermo-mechanical processing, producing a microstructure with fine, well-dispersed oxide particles. The nickel- and iron-based ODS alloys, MA754 and MA957 are two former commercially available ODS alloys (see Table 1). On the other hand the alloy HT-9, being a ferritic-martensitic grade steel, is not an ODS alloy and does not prove to be as radiation resistant. It does, however, exhibit improved strength, toughness and creep resistance at elevated temperatures up to ~400^{o}C, and shows improved void swelling resistance, which is why it has been used as a fuel cladding material in fast breeder reactors.

All the aforementioned materials are being considered for various advanced nuclear applications where traditional fusion joining processes have not been found suitable. Fusion welding of ODS alloys may cause flocculation and agglomeration of the ceramic (yttria or other derivative) oxide particles, degrading the strength of the weld zone, along with the development of porosity, inter-dendritic segregations, large tensile residual stresses [2]. The problems of conventional fusion welding is illustrated in Figure 1 showing a coarse grain structure and extensive porosity in the weld zone of a gas tungsten arc welded MA957 alloy. Some of the above-mentioned problems can also be observed as well in the fusion welding of HT-9 steels.

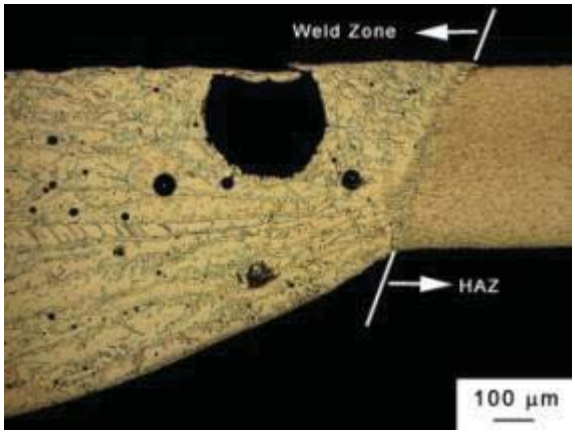

Figure 1 An optical micrograph showing a gas tungsten arc weld zone in a MA957 alloy

Thus, it is apparent that traditional fusion welding techniques are not suitable for use in joining ODS alloys and other materials for in-core applications. Hence, a solid state joining technique known as pressure resistance welding (PRW) was chosen in the present study. Very few studies on the PRW are available in the open literature L. Zirker et al [2] & M. Seki et al [3]. However, further fundamental studies are needed to fully understand the process. This paper addresses the optimization of dissimilar material joints between MA957 alloy cladding tubes and HT-9 end-plugs, having direct implications in fuel element fabrication for advanced nuclear reactors. Furthermore, results from the ongoing microstructural and crack growth studies on MA754/HT-9 alloys are highlighted.

Experimental

Materials

In this study, MA957 alloy cladding tubes having an outer diameter of 6.9 mm and HT-9 alloy cylindrical rods (also termed as the end plug) having an outer diameter of 7.9 mm were used for creating the first set of PRW welds. Also, a set of PRW welds were made between MA754 and HT-9 plates. The nominal compositions of MA957 and MA754 are given in Table 1, and the same is given for the HT-9 alloy in Table 2.

Table 1 Compositions in percent by wt.% [4]

	Fe	Ni	Cr	Mo	Ti	Al	Y_2O_3
MA754	-	Bal.	20	-	0.5	0.3	0.60
MA957	Bal.	-	14	0.3	1.0	-	0.25

Table 2 HT-9 alloy composition in wt.% [5]

	Fe	C	Cr	Mo	Mn	V	W	Ni	Si
HT9	Bal.	0.2	12	1	0.6	0.25	0.5	0.5	0.4

Weld Development

Pressure resistance welding (PRW) is basically a resistance welding technique that can be employed to perform solid-state joining of metallic materials, by carefully controlling its operational parameters. The PRW process is straightforward and is based on the simple Joule heating principle (Equation 1), coupled with a high axial joining force.

$$H = I^2 R \cdot t \quad (1)$$

Where H is taken to be the heat generated (J), I is the current (A), R is the resistance (Ω), and t is the current flow time (s). Equation 1 can be taken as true if I and R remains relatively constant for the entire length of t [6]. By controlling these variables, it is the goal of this study to obtain the most optimal weld possible.

The PRW unit utilizes a 3-phase, 60 Hz Voltza® Transgun designed and built by Centerline Ltd. based out of Windsor, Canada. The unit installed at the Center for Advanced Energy Studies (CAES-Idaho Falls, ID) is a "C" style transgun, based on the positions of the electrodes (Figure 2). The unit uses an OMHA® activator cylinder, which is responsible for the hydraulic powered force. Connected in line with the hydraulic cylinder is the electrode ram and water-cooled fixture, along with the adjacent electrode water-cooled fixture. The opposing electrode is connected to the lower electrode arm, which is linked to the transformer, completing the electron flow path. The transformer is powered by a 480 V line voltage, controlled by the welders control unit. Finally, a handheld device called the Medar, acting as the brains of the PRW, controls the welder, which programs the executable variables and records operational data.

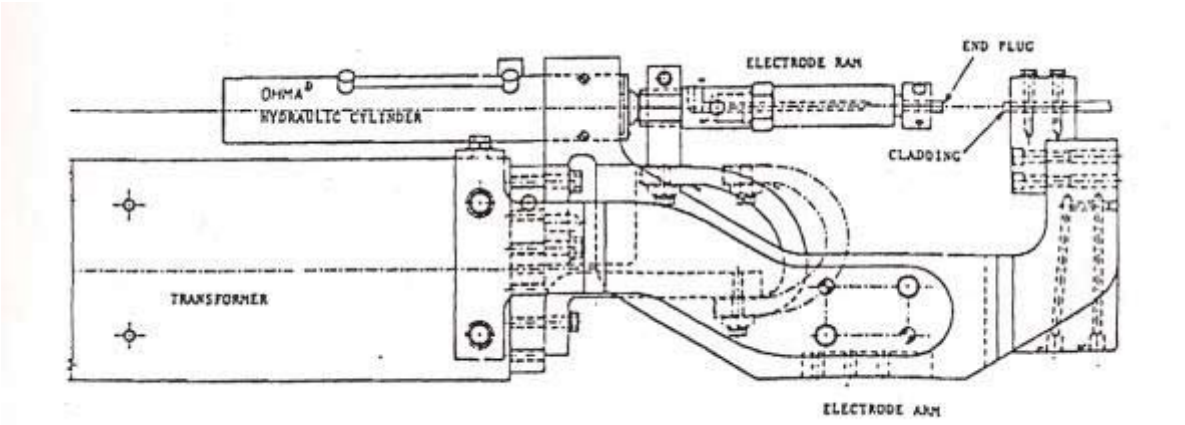

Figure2 Schematic of the "C" style Voltza® Transgun [2].

When preparing to perform a weld the specimens are placed within each electrode fixture, allowing precise protrusion lengths from the fixture surface of 2.54 mm and 1.27 mm for the end-plug and cladding tube fixtures, respectively. Once the welding cycle is initiated the electrode ram forces contact between the specimens, at about 0.689 MPa, at which time current is applied for a variable amount of time. Simultaneously, the hydraulic cylinder applies a squeeze force of about 6.89 MPa, to promote a forging of the two interfaces of the specimens. In order to minimize variability, the stick-out length and forging force has thus far been maintained, thus allowing for the current and applied time to be varied. The PRW process involves two phases, an initial softening phase where the applied current causes Joule heating of the specimens interface, and a subsequent joining phase where the secondary intensified force from the hydraulic cylinder promotes forging of the two interfaces. In this capacity, this welding method is similar to upset welding because the forging force causes the softened interfaces to experience a high degree of deformation. This deformation is deemed a quality due to the conjecture that oxidized surfaces are forced away from the final welding interface, leaving a higher quality bulk weld [6]. Once a successful weld has been completed, the specimen is categorized based on the executed variables and processed for further characterization. When the weld parameters are fully optimized to produce quality welds, further testing will be done to fully characterize the mechanical integrity of the welds. Note that the PRW joints between MA754 and HT-9 alloys were created at the Centerline facility in Windsor, Canada.

Weld Characterization

Although several characterization techniques are currently being utilized to better understand the fundamental aspects of the PRW welds, results of a few of the characterization techniques are reported here. Optical microscopy of the weld cross-sections were performed using standard metallographic practices and simple bend tests have been carried out to determine the mechanical integrity of the MA957/HT-9 PRW joints. Room temperature and elevated temperature (up to 700 ^{o}C) burst testing using internal gas (argon) pressurization in the range of 2,000-10,000 psi were performed to understand the stress-rupture properties of similarly welded joints. A view of the burst testing set-up used at North Carolina State University is shown in Figure 3.

The pressure resistance welded joints between MA754 and HT-9 plates were characterized using standard metallographic techniques at the Boise State University. The final polish of the joints was completed with a diamond slurry in a vibratory polisher. The joints were characterized using optical microscopy as well electron backscatter diffraction (EBSD) in a LEO 1430VP scanning electron microscope (SEM). The EBSD data was collected with an EDAX/TSL Digiview III detector and was analyzed with TSL Orientation Imaging Microscopy (OIM™) Analysis 5.31. The EBSD OIM™ analysis allowed for determination of grain orientation within a selected area of the sample. The specimen was tilted to 70^{o} and scanned at 25 kV accelerating voltage with a magnification between 100 and 150, which resulted in scan areas of approximately 1 mm^2. The step size of the scans was set at 2.5 μm.

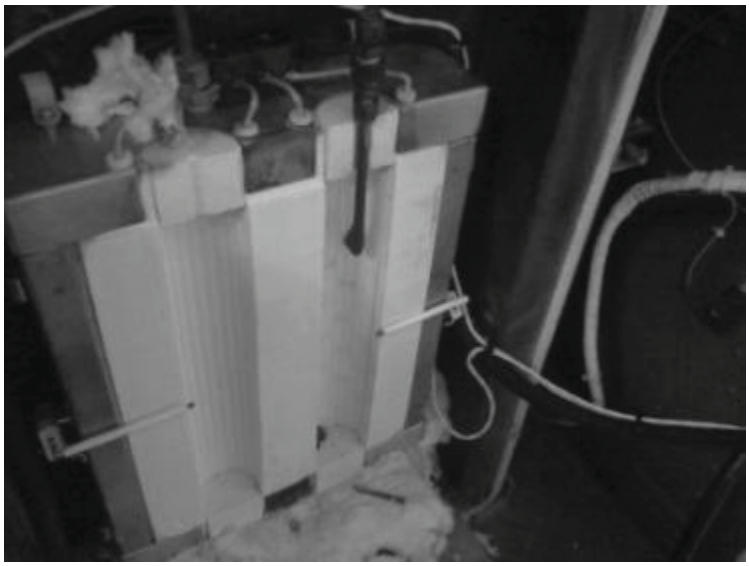

Figure 3 A view of the burst testing furnace with a failed specimen inside

Compact tension specimens were electro-discharge machined while keeping the weld interface near the crack-tip. The data attained from these tests will keep a measure of the crack growth rates of the welded specimens during fatigue cycling at constant stress intensity factor and stress ratio (R = 0.1). The direct current potential drop (DCPD) technique was used to track the crack length.

Results and Discussion

PRW of MA957 and HT-9

Process Optimization

The PRW equipment has been continuously modified to better suit requirements for this research. Numerous welds have been completed between HT-9 cylindrical end-plugs and MA957 cladding tubes, which together simulate a completed fuel pin. Although the optimization phase is still underway, optical micrographs have shown positive results. Figure 5 shows a cross-sectional view of a PRW MA957/HT-9 joint that was created at 1000 lb force, 17 kA current, 2 primary welding cycles, a hold period of 10 cycles and a final squeeze cycle of 5 cycles. These joints were also tested for mechanical integrity. These samples were first welded at the

Centerline facility in Windsor outside the scope of the ongoing weld optimization scheme. The weld zone microstructure appears to be free from any porosity and the grain structure seems to be non-dendritic. This is in contrast to what was observed in the fusion weld of MA957 alloy as shown in Figure 1. Welding of these fuel pin specimens have been completed with varying currents ranging from 7,000 to 25,000 A at varying times ranging from 33 to 55 ms. Table 3 lists weld parameters used in the ongoing optimization process and the relevant observations. As can be seen, the forging pressure and time was maintained at 800 lbs and 5 cycles (83 ms), respectively, while the current and welding time was varied. Although welding time has thus far been varied, 2 cycles (33 ms) seems to be an ideal welding time, thus allowing the effect of current to be documented, further minimizing the variability. The capabilities of the PRW are also being tested, welding with different types of current applying functions. One function includes starting at lower current inputs and increasing to a high limit over a defined time interval. Another technique includes an impulse function where current is applied a defined number of times with a defined cooling period between each impulse.

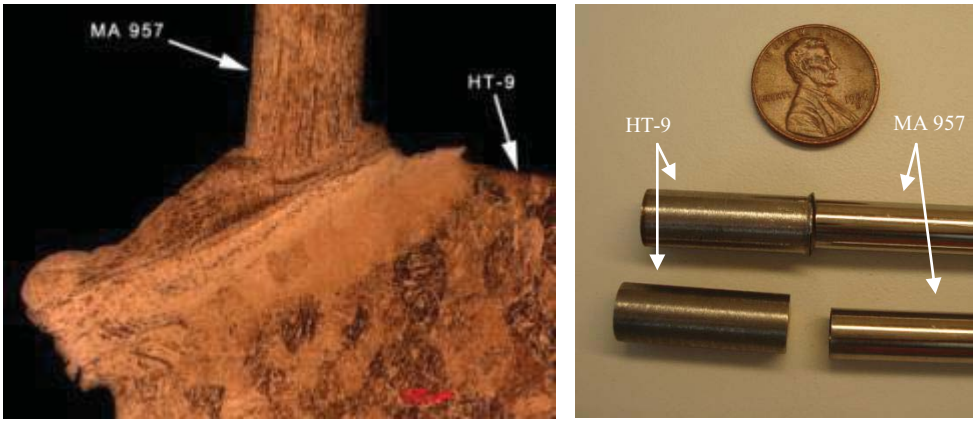

(a) *(b)*

Figure 4 a) An optical micrograph of the PRW joint cross-section. b) A MA957 tube – HT9 end plug PRW joint.

Table 3 PRW executed parameters taken from the Medar

Sample No.	Force (lbs)	Forge Time (cycles)	Weld Time (cycles)	Voltage (V)	Current (kA)	Comments
1	800	5	2	461	15.85	Welded, interface is distinguishable
2	800	5	2	471	7.34	No bonding of interfaces
3	800	5	2	465	13.52	Good weld
4	800	5	3	468	11.39	Welded, w/ slight oxidation of surface

Process Simulation

The multiphysics program COMSOL is being used to model the joule heating phenomena occurring at the joint interfaces. The fixtures and specimens have been modeled within the program, which can be used to approximate temperatures at the interfaces depending on the current and time selected. Computational analysis can be modified between the differing material specimens, based on material property inputs into the program. The forging force can also be modeled within the COMSOL program, yielding an approximate deformation of the specimens based on temperature, force and material property inputs. Overall, the COMSOL modeling is

used for preliminary approximation of possible parameter inputs of the welding control unit, to aid in determining a more fixed parameter range. A preliminary simulation view using tungsten specimens is shown in Figure 5. Further work is in progress to apply the developed simulation technique for PRW runs in ODS alloys.

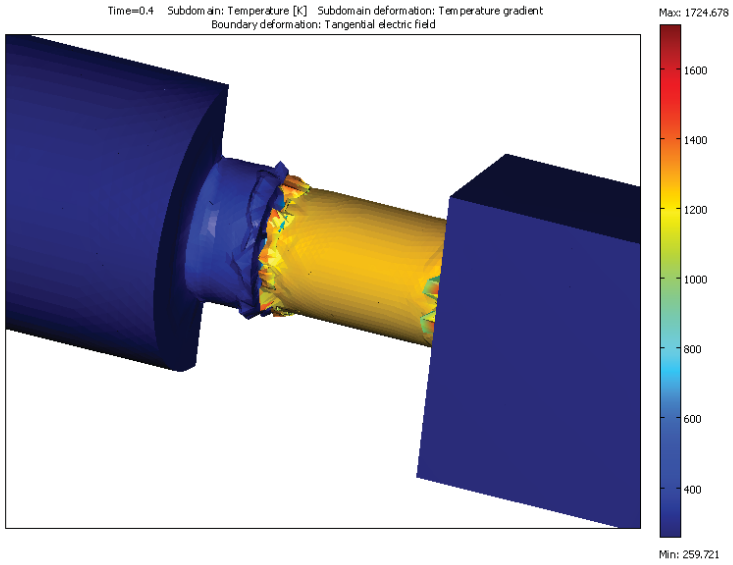

Figure 5 Preliminary simulation of joule heating within COMSOL. Force induced deformation is not included in the simulation.

Mechanical Integrity Tests for MA957-HT9 Joints

Simple mechanical bend tests were carried out on the MA957/HT-9 PRW joints. Although no quantitative properties were estimated from these tests, it demonstrated that the PRW joints were strong enough to avoid any fracture at the weld zone; even at a nearly 90^{o} bend angle. A view of two bend-tested specimens is shown in Figure 6a. On the other hand, burst testing at room temperature and up to 400 ^{o}C did not produce any rupture or any dimensional change of the cladding tubes. However, joint samples at higher temperatures did fail at the weld joint interface. A view of a failed burst specimen is shown in Figure 6b. Table 4 summarizes the burst results including relevant observations.

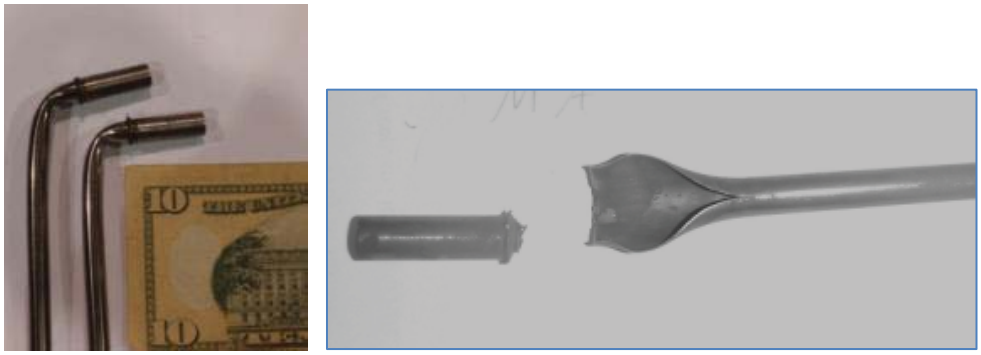

(a) *(b)*

Figure 6 (a) Two bend tested MA957-HT9 PRW joints, (b) A failed burst test specimen at 575^{o}C and a pressure of 13,000 psi.

Table 4 Summary of the burst data obtained for the MA957-HT9 joints

Test #	Temperature (^{o}C)	Pressure (psi)	Max. Uniform D (in.)	Max. Diameter (in.)	Observations
1	27	11,000	0.27	0.27	No change
2	400	11,000	0.27	0.27	No change
3	390	11,500	0.27	0.27	No change
4	390	14,500	0.27	0.27	Held for 4977 min
5	575	13,000	0.271	0.651	Weld failed, held for 9 min
6	650	8,000	0.299	0.703	Weld failed, held for 1 min
7	700	8,000	0.304	0.712	Weld failed at < 1 min
8	750	5,000	0.297	0.674	Weld failed after 30 s
9	781	4,000	0.311	0.421	Weld failed after 45 min
10	812	4,800	0.308	0.491	Weld failed during the initial pressurization stage

PRW of MA754 and HT-9

Several PRW joints between MA754 and HT9 joints (21 in total) were created. They appeared as shown in Figures 7a and 7b. Seven of the best samples were selected for further mechanical evaluation. Each of the seven samples were machined into compact tension specimens (CTS) using a wire electrical discharge machining (EDM) method with a 10 μm wire as shown in Figure 8a. This geometry was chosen in order to evaluate the crack propagation behavior using the linear elastic fracture mechanics (LEFM) principles. Ideally, the machined crack tip would be at the center of the weld interface to allow the crack to initiate at the weld interface. However, due to the non-linear nature of the weld interface, aligning the machine-cut to the weld interface proved difficult. Figure 8b shows a corresponding conventional SEM image of the polished cross-section of the joint containing the crack tip.

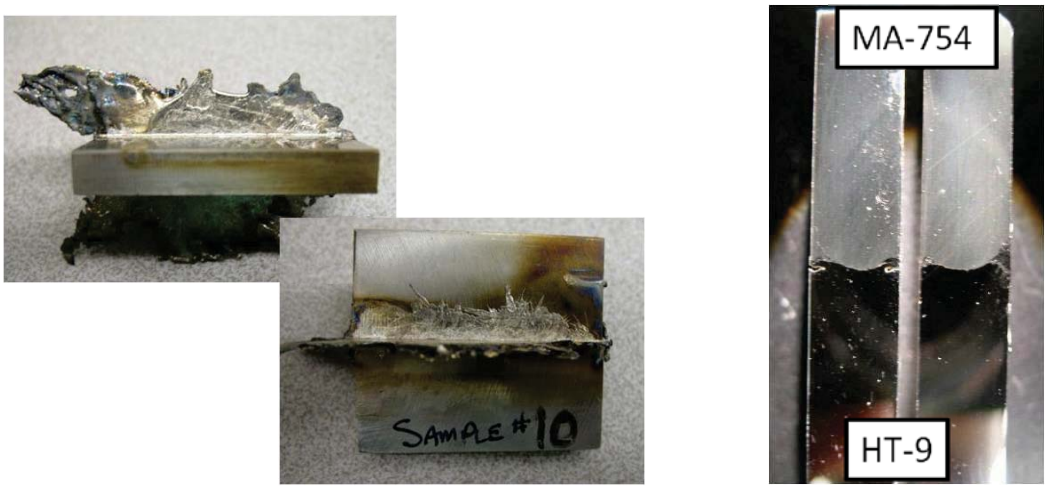

(a) *(b)*

Figure 7 Macro-images of HT-9 to MA-754 joints created by pressure assistance welding. a) As-received joint showing the "flash" material. b) The polished cross section of the samples showing the HT-9 and the MA-754 sides of the joint and the profile of the weld.

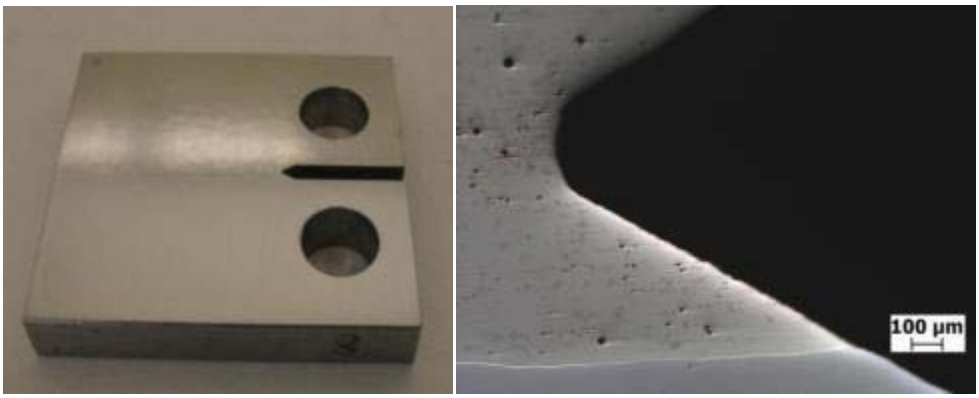

Figure 8 a) Image of a HT-9 to MA-754 PRW crack test specimen after polishing with a 6 µm diamond slurry. The specimens were machined using a wire EDM technique to give precise crack tip geometry (shown by the SEM image of (b)) and a high tolerance mechanical test specimens. Notice the position of the joint relative to the crack tip.

Prior to conducting the fatigue crack experiments, the microstructure of a joint sample was evaluated using the EBSD technique. The SEM and corresponding EBSD images are shown in Figure 9. Given that the surface preparation is unique for each type of material and very important when using EBSD techniques, much time and effort were invested to provide sufficient relief for each of the two material surfaces without using a chemical etch (due to the adverse effects of the etch in the void space and the crack tip). The sample was first polished to 1200 grit using polishing cloths and diamond paste prior to being placed on a vibratory polisher in a colloidal silica slurry for 18 hours. Figure 9a shows a low magnification SEM image of the crack tip of the CTS. A nickel phase was chosen for indexing the corresponding EBSD image (Figure 9b). It should be noted that the confidence levels near the crack tip are relatively high but reduces as the distance from the crack tip increases. Also, not all of the specimen could be indexed due to the fact that iron phases were not indexed. Details of the fatigue crack experiments and further results will be published elsewhere. While more crack growth tests are currently ongoing, the specimen imaged above failed after about 4000 cycles.

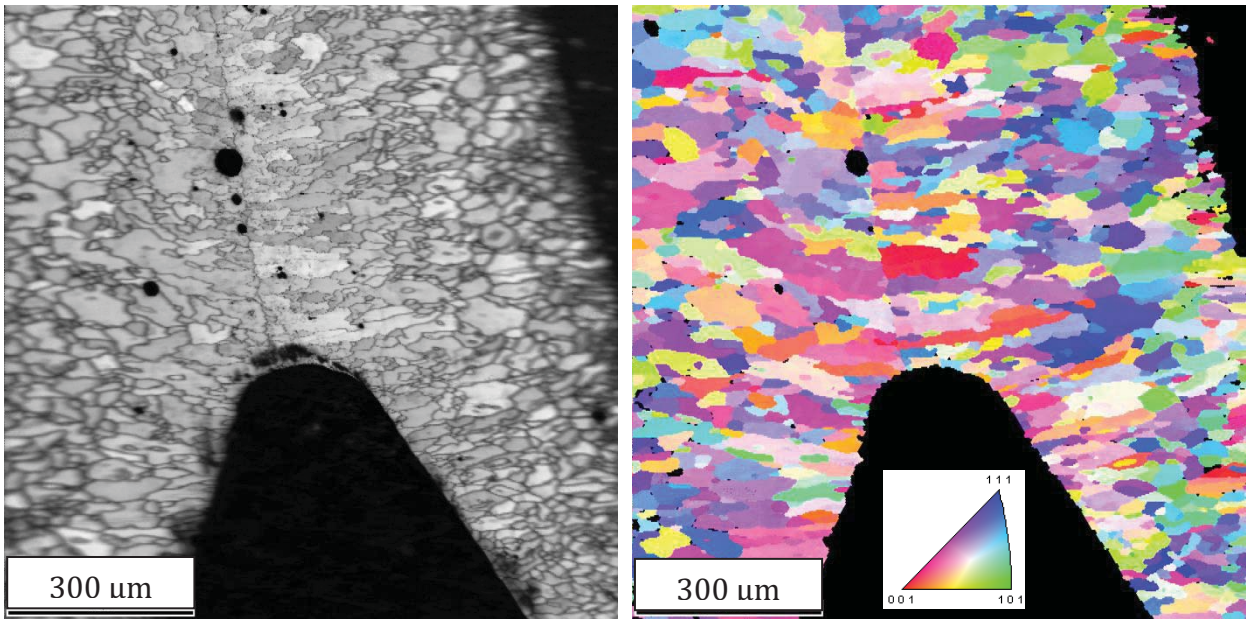

(a) (b)

Figure 9 Microstructure of the HT-9 to MA-754 PRW joint. a) EBSD inverse pole figure map indexing the present nickel phase and b) the corresponding Kikuchi pattern quality map of the machined crack tip of a joint in a CTS.

Summary and Concluding Remarks

This paper discusses the solid state weldability characteristics between ODS alloys (MA957 and MA754 alloys) and HT9 steel through pressure resistance welding. The initial results indicate the joint created are mostly sound. Burst tests and simple bend tests of the MA957-HT9 joints were performed. They showed encouraging results. However, at elevated enough temperatures at higher pressures, failure of the joints occurred. Microhardness testing will be performed on the joints to assess the hardness gradients. EBSD studies have been performed on the MA754 and HT-9 alloys. The EBSD sample preparation proved to be a challenging task. Fatigue crack growth experiments are ongoing to better understand the fatigue crack resistance behavior of these joints. Experimental studies along with COMSOL simulation are expected to help optimize the welding process and lead to further progress in this area.

Acknowledgments

We gratefully acknowledge the support of the US Department of Energy and the Idaho National Laboratory for this research. Nathan Jerred would like to thank the Idaho Space Grant Consortium (ISGC) for a graduate fellowship awarded to him. Also, we wish to thank Tyler Alexander and Mark Woltz of the Centerline Limited and Kalyan Chitrada of the University of Idaho, for their contributions.

References

[1] Murty, K.L. and Charit, I. “Structural Materials for Gen-IV Nuclear Reactors: Challenges and Opportunities,” 383 (2008) 189-195.

[2] Zirker, L., Shikakura, S., Tsai, C., and Hamilton, M., “Fabrication of Oxide Dispersion Strengthened Ferritic Clad Fuel Pins.” Proc. of International Conference on Fast Reactors and Related Fuel Cycles, Kyoto, Japan.

[3] Fischer, J., and Haeberle, R., “Commercial Status of Mechanically Alloyed Materials.” *Modern Developments in Powder Metallurgy*, Vol. 21, Proc. Of International Powder Metallurgy Conference, Orlando, Florida, p461.

[4] Seki, M., Mirako, K., Kono, S., Kihara, Y., Kaito, T., and Ukai, S., “Pressurized Resistance Welding Technology Development in 9Cr-ODS Martensitic Steels," *Journal of Nuclear Materials* 329-333 (2004) 1534-538.

[5] Klueh, R. "Ferritic/Martensitic Steels for Advanced Nuclear Reactors." *Transactions of the Indian Institute of Metals* 62 (2009) 81-87.

[6] "Procedure Development and Process Considerations for Resistance Welding." *ASM Handbook: Welding, Brazing & Soldering*, Vol. 6, 833-850.